Journal of Materials Research and Technology 32 (2024) 1152–1158

Contents lists available at ScienceDirect

Journal of Materials Research and Technology

journal homepage: www.elsevier.com/locate/jmrt

How to achieve nanometer flat surfaces: Pulsed electrochemical machining of bulk metallic glass

Bastian Adam [a,*], Thomas Hall [b,c], Lucas Matthias Ruschel [a], Florian Schäfer [d], Christoph Pauly [e], Dirk Bähre [b,c], Ralf Busch [a]

[a] Chair of metallic materials, Saarland University, Campus C6.3, 66123, Saarbrücken, Germany
[b] Institute of Production Engineering, Saarland University, Campus A4 2, 66123, Saarbrücken, Germany
[c] Center for Mechatronics and Automation Technology (ZeMA gGmbH), Gewerbepark Eschberger Weg 46 Gebäude 9, 66121, Saarbrücken, Germany
[d] Dept. Materials Science and Methods, Saarland University, Campus D2 3, 66123, Saarbrücken, Germany
[e] Dept. Materials Science and Engineering, Saarland University, Campus D3 3, 66123, Saarbrücken, Germany

ARTICLE INFO

Handling editor: P.Y. Chen

Keywords:
Bulk metallic glasses
Pulsed electrochemical machining
BMG post-processing
Superior surface quality

ABSTRACT

The Bulk Metallic Glass (BMG) Vitreloy 105 ($Zr_{52.5}Ti_5Ni_{14.6}Cu_{17.9}Al_{10}$) as well as two crystalline reference materials of the same composition were machined with Pulsed Electrochemical Machining (PECM). One reference material was nano crystalline with an average grain size of 11 nm and the second one was a fine grain crystalline sample with an average grainsize of 110 nm. The goal was to achieve maximum surface quality in terms of roughness by utilizing a readily available industrial process. Samples were characterized by tactile profilometer, atomic force microscopy and electron microscopy methods. The results show superior surface quality of the amorphous samples over the reference materials with an average roughness depth as low as 1 nm. The observed dissolution mechanism of the BMG differs from the reference materials -as in contrast to the crystalline alloys that show a passive layer formation - no such surface layer other than the native oxide could be observed. The PECM procedure is found to be a promising post-processing step for BMGs with a resulting surface that can face even the most challenging surface quality requirements.

1. Introduction

Amorphous metals or metallic glasses are rapidly quenched alloys that form glass upon cooling from the melt rather than crystallizing. These metallic glasses have been the objective of current research activities due to their unique properties. Bulk Metallic Glasses (BMGs) are metallic glasses that can be quenched into the amorphous state in dimensions beyond 1 mm thickness [1]. The Vitreloy 105 alloy ($Zr_{52.5}Ti_5Ni_{14.6}Cu_{17.9}Al_{10}$) was developed in the early 1990's as part of the Vitreloy family that was produced by Liquid-metal Technologies and comprises also well-known alloys like the Vitreloy 101, Vitreloy 104 and Vitreloy 106 [2]. This composition shows a good glass forming ability paired with interesting mechanical properties of a high yield strength [3] and ductility in bending [4], as well as in compressive testing. The alloy also shows a high fracture toughness, depending on specimen size [5] and thermomechanical treatment [6]. The alloy is produced on an industrial scale by special alloy manufacturers - for injection casting of commercial parts and additive manufacturing solutions. Thus, the alloy was chosen as the initial candidate for this study on macroscopic Pulsed Electro Chemical Machining (PECM) of BMGs. PECM is a contactless manufacturing process utilizing pulsed anodic metal dissolution in a flowing electrolyte environment. The limiting factors of the processing method often lie within the processed material itself as the microstructure and its inhomogeneous dissolution restricts the surface quality [7]. The machinability of BMGs by PECM was demonstrated in 2021 [8] in the form of micro-machining dimple patterns on the Vit105 alloy. The dissolution mechanism was reported by Guo et al. where they show that the polarization behavior follows "active dissolution and valve metal passivation" which incorporates an initial Pitting/Oxidation step, followed by a supersaturated film formation and the establishment of a continuous polishing effect induced by the supersaturated film "which finally resulted in the uniform dissolution of Zr-based BMG" [8]. For the macroscopic PECM, the roughness of the resulting surface is dependent on the machining parameters, with a reproducible, high quality polish generating processing window of employed current densities that was reported by Hall et al. to be found between 90 A/cm^2 and 125 A/cm^2

* Corresponding author.
E-mail address: bastian.adam@uni-saarland.de (B. Adam).

https://doi.org/10.1016/j.jmrt.2024.07.130
Received 14 May 2024; Received in revised form 8 July 2024; Accepted 21 July 2024
Available online 26 July 2024

[9].

Post-processing is necessary for BMG parts, since this class of materials, due to the absence of typical features of crystalline materials such as grains or grain boundaries, shows a near ideal replication of the mold's surface in the casting's surface, thereby allowing near-net-shape during injection casting [9]. However, the replication also transfers to smallest imperfections and wear deformation of the molds, which is not quite favorable even for small series production. An alternative manufacturing route is thermoplastic forming in the supercooled liquid state that can also replicate smallest details of the respective mold used during the thermoplastic forming. Therefore, both the casting as well as the thermoplastic forming rely on the quality of the molds and tools employed in the process [10]. Alternatively, the manufacturing route of thermoplastic forming in the supercooled liquid state can also replicate smallest details of the respective mold used during the thermoplastic forming [11].

The PECM offers the possibility to reduce the impact of mold and tool quality by machining the BMG parts contact-less to a high surface quality. This is getting even more important, as additive manufacturing makes up a large part of the recent research on metallic glasses, which is usually accompanied by a post-processing procedure to enhance the surface quality of the rather rough additively manufactured surface [12]. For any decorative application or jewelry, post-processing is especially important as the surface finish quality requirements are challenging in the high-performance part industries.

2. Materials and methods

2.1. Synthesis and sample analysis

The ingots of the composition $Zr_{52.5}Ti_5Ni_{14.6}Cu_{17.9}Al_{10}$ were produced in an arc melting furnace under protective 99.999 vol% (5 N) argon atmosphere, using 99.99 wt% (4 N) pure metallic materials. These master alloys were then used to produce amorphous specimens by arc melting and suction casting under Ti-purified 5 N argon atmosphere into water cooled copper molds. Their amorphous structure was verified by X-ray diffraction (XRD) on a D8-A25-Advance diffractometer in Bragg-Brentano θ-θ-geometry (goniometer radius 280 mm) in a 2θ range of 20–80° with Cu K_α-radiation ($\lambda = 154$ p.m.). The size of the respective primary phases was determined with the Bruker TOPAS software utilizing volume-weighted lognormal size distribution of crystallites (LVOlB) methodology. Differential thermal analysis was performed with a Netzsch STA 449 F3 Jupiter and a heating rate of 20 K/min in Y_2O_3 coated graphite crucibles under constant flow of high purity 6 N argon purge gas.

2.2. Pulsed electrochemical machining (PECM)

For PECM processing, the stainless-steel tool with a diameter of 5 mm was fed into the aligned Vit105 workpiece with a diameter of 3 mm. Dissolution behavior was recorded with iteratively varied feed rate and the corresponding surface quality at different current densities is assessed. The experiments were performed in a PA2200 flushing chamber that ensures constant electrolyte rinsing. A PEM-Center 8000 (PEMTec SNC, France) fitted with sodium nitrate-based electrolyte with a conductivity of 100 ± 5 mS/cm was used for the electrochemical material characterization. The physical setup and abstract procedure visualization can be seen in the supplementary file in Fig. 1 a) and b).

The total removal of material was situated between 0.5 mm and 1 mm in length depending on the specific material removal rate (SMR), thereby removing the initial topography that was rough sawn ($R_a > 10$ μm) from the cut with a metallographic Presi Mecatome T202 precision saw for all samples and considered insignificant due to the considerable mass removal of the process. The process was performed at 12 V process voltage, with 5 s of pulse-on time with a mechanical and electrical frequency of 50 Hz. The electrolyte was kept at a temperature of 20 °C and the electrolyte pressure was held at 200 kPa to maintain a stable flow during the machining process. Parameters of the PECM process were kept within the previously published functional processing windows for amorphous Vit105 of reference [9], this includes current densities, pulse time, pulse form as well as electrolyte concentration and feed rate identical to Fig. S1 and samples result from an optimal current density range postulated in Supplementary Fig. S5.

2.3. Annealing procedure for crystalline reference material

To compare the PECM process of amorphous samples to the crystalline counterpart, amorphous Vit105 references were crystallized by conducting two different annealing procedures under 5 N argon atmosphere. Two sets of crystalline reference samples were prepared by annealing, one nano crystalline reference set, from an amorphous precursor annealed at 723 K for 12 h and a fine grain reference set at 1003 K (50 K below the beginning of melting), which was also annealed for 12 h and is considerably coarser than the nanocrystalline material.

2.4. Electron microscopy

Scanning electron microscopy (SEM) was performed on a Zeiss Sigma

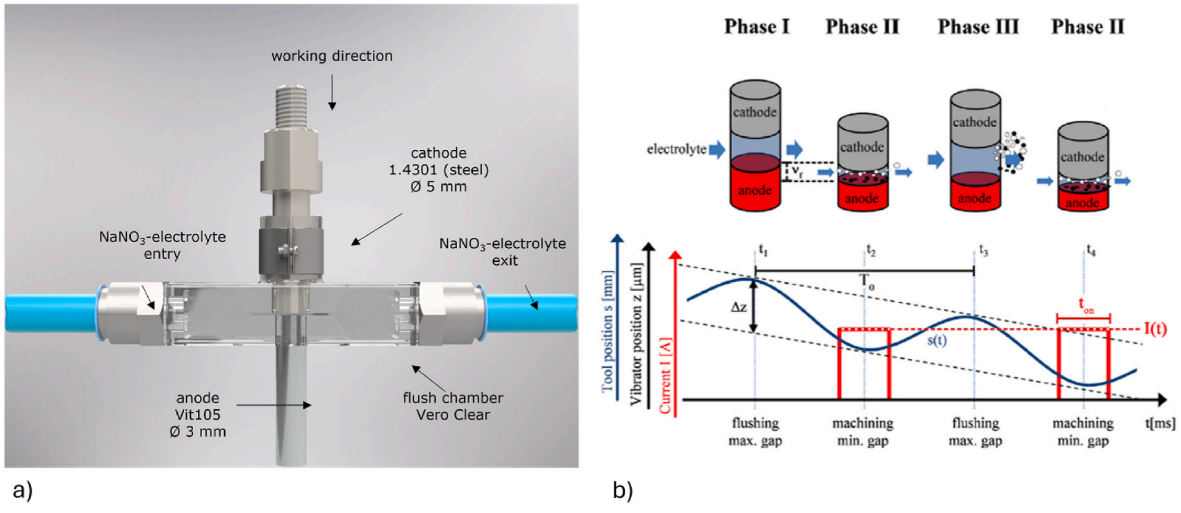

Fig. 1. a) schematic setup of the PECM procedure and b) working principle of the PECM method by Weber et al. [13], reprinted under copyright license 5838151066046.

VP FEG-SEM as well as on a FEI Helios NanoLab600, where also the focused ion beam machining (FIB) took place. Acceleration voltages ranging from 5 kV to 30 kV were applied during the imaging. Contrast modes include backscattering images (BSE), secondary electron images (SE), and scanning transmission mode images (STEM).

TEM lamellae were prepared by Focused Ion Beam (FIB) machining with Ga ions and after lift out the lamellae were investigated on a JEOL Type JEM2011 TEM at an acceleration voltage of 200 kV.

2.5. Surface analysis

The surface evaluation was carried out in the first step by tactile measurement on a perthometer MarSurf XR/XT20. Furthermore, atomic force microscopy was performed on a Bruker Dimension Icon using ScanAsyst Mode with ScanAsyst Air tips from Bruker Inc. An area of 10 × 10 μm^2 was probed with an image resolution of 512x512 pixel. From the AFM topography data, the statistical roughness values were determined with the Gwyddion 2.61 software [14].

3. Results

The thermogram of the DTA scan for Vit105 is displayed in Fig. 2 a) with arrows indicating the temperatures, at which the reference samples were held isothermally to set different crystallization stages. The corresponding XRD diffractograms of the as-cast reference, the samples after PECM machining as well as the annealed samples are show in Fig. 2 b). Annealing for 12 h at 723 K yielded a nano crystalline sample, containing primarily a Zr_2Ni type structure (Powder diffraction file (PDF) 00-038-1170) [15] and the second annealing procedure for 12 h at 1003 K yielded a fine-grain sample comprised of a mixture of Zr_2Cu (PDF 00-018-0466) [15] and remaining Zr_2Ni type in the microstructure plus an additional minor phase that could not be identified, the diffractograms are depicted in detail in Fig. 2 b). The microstructure is here dominated by the primary phases, the TOPAS LVolB analysis of the XRD spectra results in a determined crystallite size of 11 nm ± 1 nm for the nano crystalline sample that was 12 h annealed at 723 K and a crystallite size of 110 nm ± 10 nm for the fine-grain sample, annealed for 12 h at 1003 K. The SEM images of the FIB prepared lamellae showing the resulting microstructures are depicted in the supplementary file in Fig. S4.

The as-cast state and the pulsed electrochemically machined Vit105 rods are X-ray amorphous as can be seen by the respective diffractograms, where both the as-cast material as well as the machined Vit105 rod show only a broad amorphous halo without any presence of crystalline Bragg reflexes. This confirms that the method is suitable for processing metallic glasses without altering the amorphous structure as it can easily happen during conventional processing that introduces heat into the workpiece during machining. Optical inspection of the surface with scanning electron microscopy yielded rather differing topographies, Fig. 3 a) depicts a close up of the surface from an amorphous 3 mm diameter rod after the PECM processing - the surface appears to be smooth, containing little waviness. Fig. 3 b) shows the surface of the nanocrystalline sample which shows a distinct structure within the surface and in Fig. 3 c) the fine-grain sample is depicted which is significantly coarser than the surface of the amorphous sample. The surface quality of the crystalline samples after PECM seems to be dominated by the dimensions of the respective microstructure. The secondary electron image of Fig. 3 b) depicts a partially excavated nanometer-scaled structure for the 12 h at 723 K annealed sample and an overall rougher topography compared to the amorphous sample. The sample annealed for 12 h at 1003 K in Fig. 3 c), however, shows a coarse and partially dissolved fine-grain microstructure. The surfaces displayed in Fig. 3 a)-c) were FIB cut and the images are displayed in Fig. 3 d)-f) where the difference between the amorphous sample (d), the low temperature annealed sample (e), and the high temperature annealed Vit105 samples (f) can be seen. The crystalline samples seem to feature

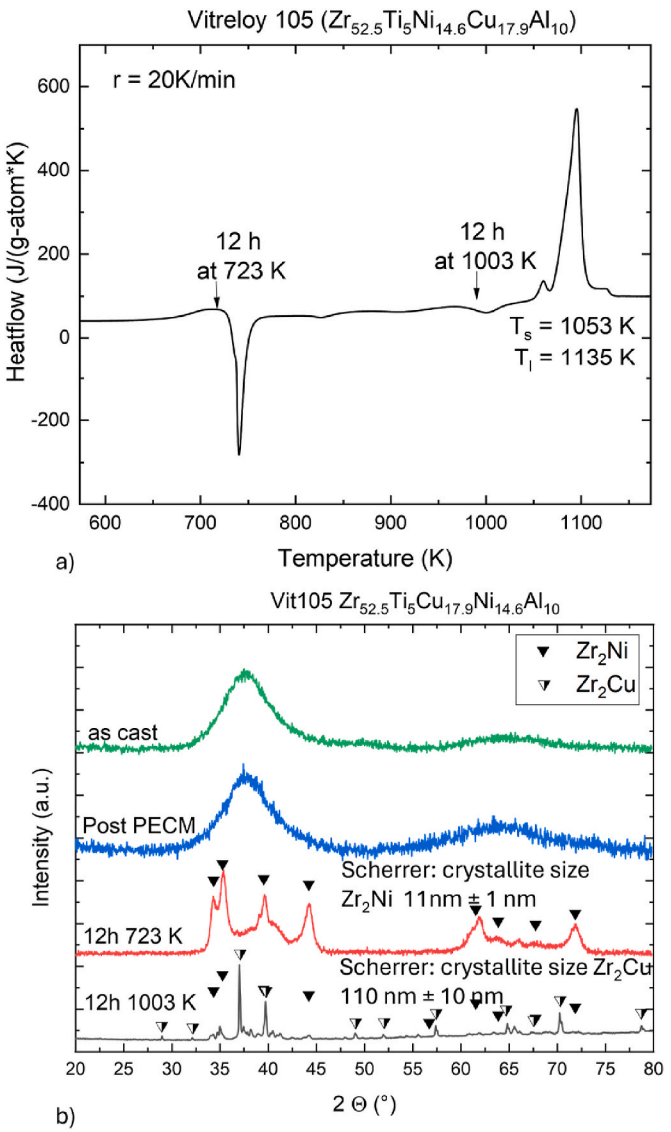

Fig. 2. a) DTA thermogram of the Vit105 alloy with marked annealing procedures in the SCLR as well as close to the solidus temperature of the Vit105 alloy. b) XRD results of as cast Vit105 material before and after pulsed electrochemical machining on a 3 mm diameter rod sample showing no significant structural change during machining. The annealing procedure indicated in a) results in different crystalline configurations, primarily Zr_2Ni and Zr_2Cu compounds.

an oxide/corrosion layer after PECM, with a thickness measuring 18 ± 5 nm for the sample annealed at 723 K and 35 ± 18 nm for the sample annealed at 1003 K. Such a surface layer cannot be detected for the processed amorphous sample by SEM alone. In addition, the high temperature annealed sample (1003 K) also shows significant holes in the surface, where parts of the microstructure were dissolved faster, resulting in pits. The optical color of the samples is also different, while the amorphous and low temperature annealed sample appear metallic and highly reflective, the high temperature annealed sample has a dull blackish grey surface appearance.

For the amorphous material, the smooth transition was further investigated by TEM imaging and the result can be seen in Fig. 4 where the higher magnification of the TEM shows a smooth interlayer between the applied Pt and the bulk sample. The dissolution layer is here significantly thinner than in the crystalline counterparts, as it cannot be easily distinguished where the layer ends and where the deposited Pt starts due to optical artifacts resulting from the tilt and sample thickness,

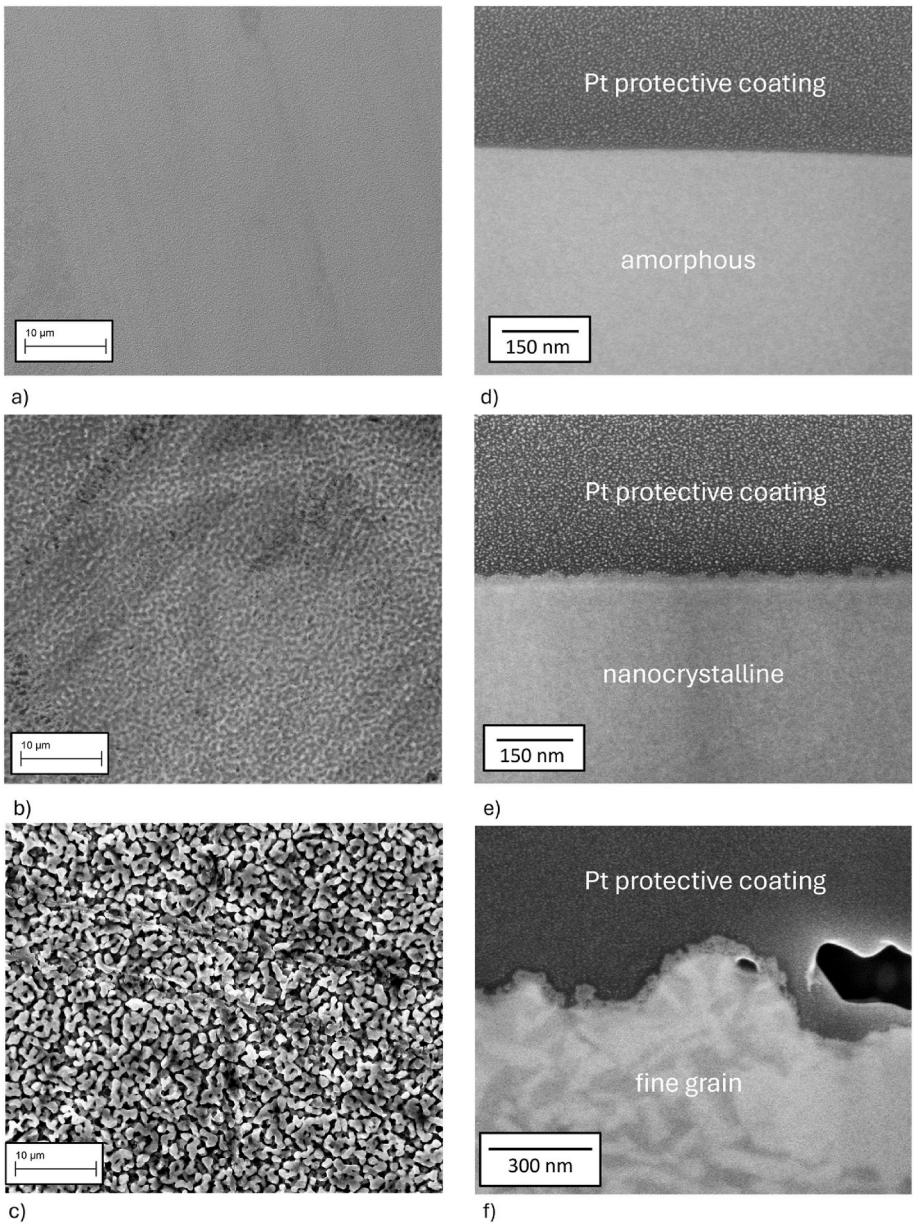

Fig. 3. a) Overview secondary electron contrast image of the surface of the amorphous Vit105 rod after pulsed electrochemical machining that shows a smooth surface with almost no contrast in the SE2 imaging b) the surface after pulsed electrochemical machining of the nano crystalline sample that was annealed for 12 h at 773 K and c) the resulting surface of the PECM on the fine-grain crystalline sample that was annealed for 12 h at 1003 K d) Surface of the amorphous Vit105 sample in a FIB cut cross-section showing a smooth surface that was coated with Pt e) a FIB cut of the 12 h at 723 K annealed sample f) FIB cut of the 12 h at 1003 K annealed sample, showing a much rougher surface and multiphase microstructure. All FIB-SEM images d)-f) were taken under 52° sample tilt.

however it can be derived that the layer is smaller than 10 nm in thickness and therefore the surface layer is significantly thinner than that of the crystalline counterparts.

The surface was further analyzed by atomic force microscopy, where an area of 10 µm × 10 µm was probed. The recorded image with a maximum height-contrast of 44.1 nm can be seen in Fig. 5 a) for the amorphous sample, where the height-contrast results mainly from singular particles, as most of the surface is located below a height-value of 25 nm. The average maximum roughness depth R_Z was measured as 8.2 nm over a measured length of 12 µm.

In comparison with the low temperature annealed sample shown in Fig. 5 b) and the high temperature annealed sample depicted in Fig. 5 c) the measured roughness of the low temperature annealed sample is close to that of the amorphous sample, although there is a significant difference in the determined mean roughness depth R_z, yet both are in the order of a few nanometers and mostly below 25 nm.

4. Discussion

Smooth and reproducible surfaces of high quality are a desirable feature for all workpieces produced by injection casting. Here, a cost efficient and readily available industrial process is used for the post-processing of amorphous workpieces, independent of the initial surface quality. The PECM post processing takes away the need for high quality molds and tools, as the surface quality reached by PECM is significantly higher than the quality a directly cast BMG could reach in a realistic production setup while also possessing significantly longer tool life due to the contactless machining. Realistic production set up means here, that the mold is made from a conventional crystalline material like tool steel or copper, which wears out inevitably due to the harsh casting

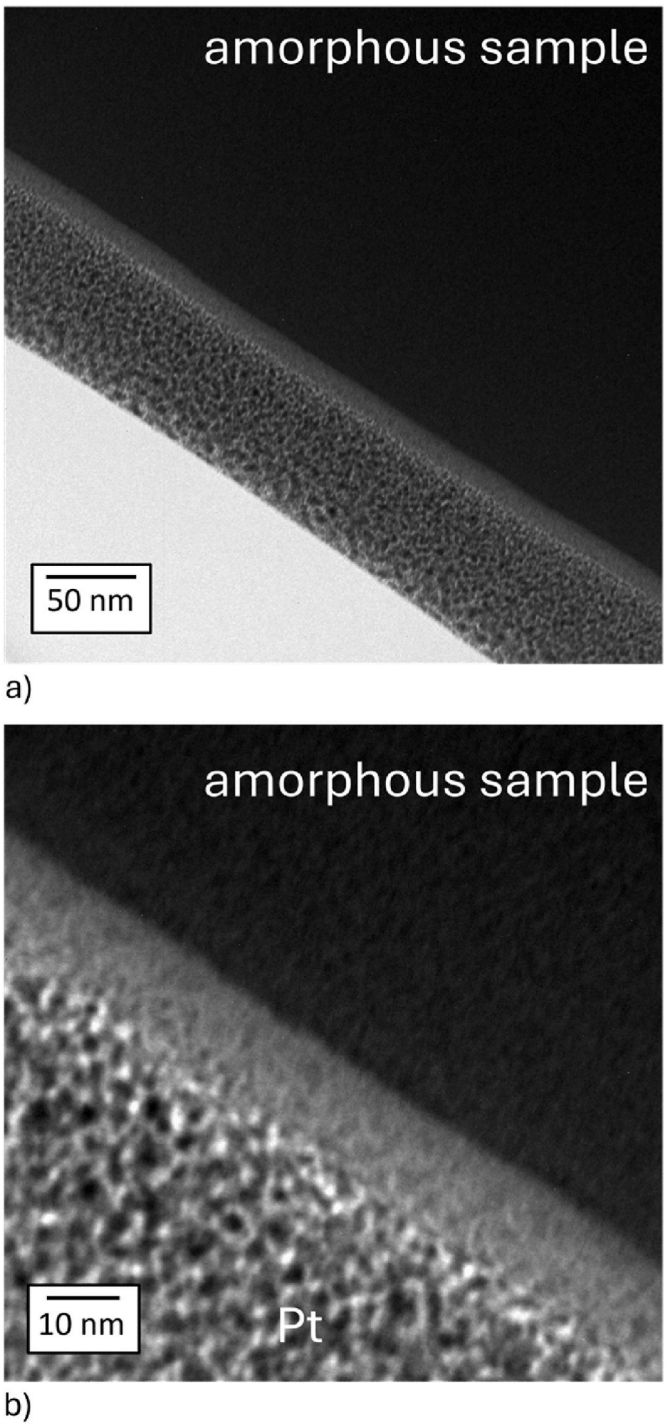

Fig. 4. a) TEM bright field image showing the amorphous samples surface cross-section, consisting of covering Pt on the surface of the PECM processed sample, an interlayer where the Pt is deposited and the bulk amorphous sample b) higher magnification of the interlayer section where the Pt is deposited on the PECM processed amorphous samples surface.

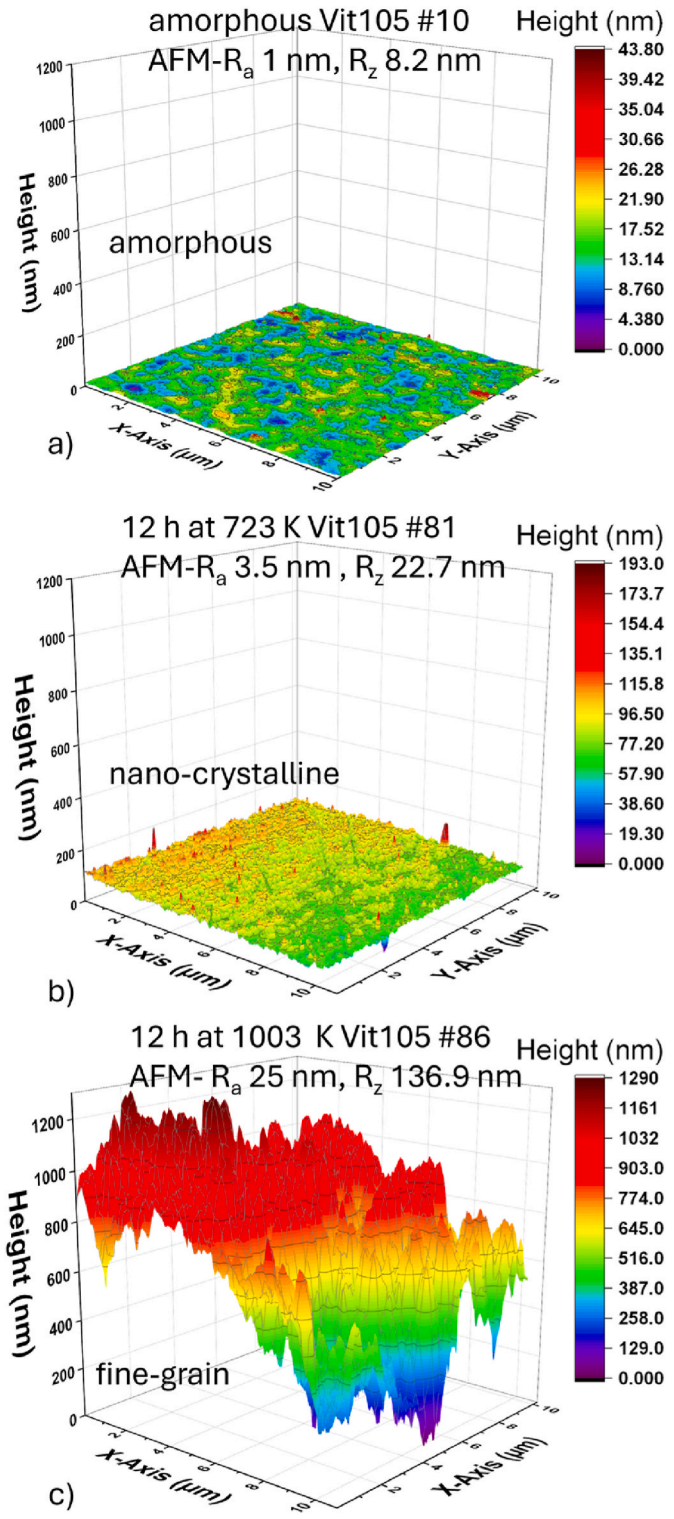

Fig. 5. AFM image of 10 μm × 10 μm area where a representative absolute height scale is given for all 3 subfigures and a relative color coding for the relative height differences within each individual surface. In the following order of a) amorphous Vit105 after the PECM process b) 12 h annealed at 723 K nano crystalline Vit105 c) 12 h annealed at 1003 K fine-grain material.

conditions of BMG alloys and transfers even smallest flaws into the cast parts.

Table 1 summarizes the results of the different roughness characterization methods and presents the respective significant processing parameters for the different structural states. The results signify that the PECM method seems - in this case - to be only limited by the microstructure of the processed material for optimized parameters sets, which in case of the amorphous material could reach down to the amorphous short-range order or the respective size of the clusters. Therefore, the correlation that was stated by Kozak et al. for Ti-based materials [7] appears to hold true also from fine-grain material (crystallite size 110 nm) over nanocrystalline material (crystallite size 11 nm) down to the medium range order that poses as the significant upper size limit of

Table 1
Specific parameter sets of the three presented samples as well as the determined roughness by perthometer and atomic force microscopy.

sample			PECM			Perthometer			AFM		
			parameter			line-profile 1.25 mm			line-profile 12 μm		
Nr.	structure	state	v_f (mm/min)	loss (mg)	time (s)	R_a (nm)	R_z (nm)	λ_a (nm)	R_a (nm)	R_z (nm)	R_z ISO (nm)
10	amorphous	as-cast	0.75	70	132	11	60	201.3	1	8	6
81	nanocrystal	12 h 723 K	0.7	98	172	27	120	206.2	3.5	24	23
86	fine-grain	12 h 1003 K	0.7	75	147	250	1528	431.7	23	142	137

"structure" for the amorphous phase (sub 1 nm), that the achievable surface roughness is directly correlated to the size of the respective microstructure. In the case of amorphous Vit105 a reproducible average roughness R_a below 25 nm was reached and verified with AFM measurements while the found R_z values were in a range below 100 nm. The difference in AFM and perthometer absolute roughness values results likely from the significantly larger profile that is probed by the perthometer, yet the methods both show the same trend between the materials and depict a high surface quality.

PECM can therefore readily be used to rework BMG parts, where defects like surface porosities, flow serrations and similar faults can be frequently encountered which limit the obtainable surface quality. PECM can pose a useful alternative -given the part has enough Glass forming ability to add a reasonable allowance in material thickness. Table 2 shows the roughness classes of the classical Swiss watchmaking standard NIHS 07-02 which is based on the DIN EN ISO 1302 and sets the PECM processing of amorphous Vit105 alloy in relation to common automated polishing preparations.

Conventional post-processing is limited by the tool and mold quality for BMGs during casting itself or the subsequent thermoplastic forming route that can also achieve high quality surfaces [11]. The achievable surface quality with a macroscopic R_a value below 25 nm and R_z value below 100 nm [9] of the PECM can be roughly compared to metallographic preparations with 3 μm diamond polishing. The process is in comparison quite fast, as the machining of the samples was performed within 3 min of PECM each. While regular polishing for non-flat samples can take several hours up to days depending on the material, polishing agent, and the number of polishing steps the PECM is thoroughly able to shape the workpiece and process the surface within the same operation.

Albeit the crystalline reference materials can reach similar surface qualities for fine scale nanocrystalline materials in this study, the surface quality of even fine-grain material is limited due to the inhomogeneous dissolution of the multiphase microstructure. Furthermore, crystalline materials show a passivation/oxidation layer that builds up during the processing that is not encountered in a significant or evident thickness during processing of amorphous Vit105. Meaning that within the methods of this study, the resulting surface layer of amorphous Vit105 could only be determined to possess a thickness below 10 nm, which is quite close to the range of 1–10 nm of native oxide on Zr as reported by Bakradze when growing Zr-oxides on bare Zr during controlled oxygen exposure [16]. To us, this indicates that the mechanism of dissolution differs between amorphous and crystalline material within the same PECM parameter range due to the difference local structure and difference in chemical homogeneity, highlighting the importance to further study the electrochemical dissolution mechanism of BMG under PECM processing conditions.

5. Conclusion

The investigated method of PECM on BMG parts produces optically reflective surfaces with a high quality surface finish that falls into the highest standards of even watch makers grade N1 when probed by tactile measurements and able to reach single digit nm average and maximum roughness depth in the AFM -an average depth of roughness of 1 nm can be probed with the AFM, accompanied with a maximum roughness depth of 8 nm. This can be confirmed with the roughness value results of tactile perthometer measurements. Therefore, a direct correlation between the size of the microstructure and the resulting surface roughness can be stated as from the amorphous over the nanocrystalline to the fine-grain Vit105 alloy, it is found that the larger the particles/structures within the microstructure are, the higher was the resulting roughness of the PECM processed surface.

The amorphous structure of the BMG parts remains unchanged by the process as the low process temperature and contactless machining already suggests and furthermore there is no significant buildup of corrosion or dissolution layers on the surface of the amorphous sample for the selected parameter range. The investigation is to be seen as starting point for further studies of PECM on BMG and the authors plan to expand similar investigations into chemically different families of BMG like the Cu-based or the Ni-based BMG systems. Previous studies on micro-machining via PECM and surface texturing workpieces even with functional structures [17] have been reported, also novel fabrication methods for micro-structured tools have been investigated [18] and pose new possibilities for innovative manufacturing with BMG materials.

The combination of Bulk Metallic Glasses and PECM enables the technology to be explored without the restrictions of a hindering microstructure with its inherent defects and grain boundaries and focus on the exploration of the production engineering capabilities from the bulk material. The electrochemical machining itself is a well-developed manufacturing technology with recent innovative advances even opening the possibilities "to meet the requirements of high precision, high surface integrity, high efficiency and high economic affordability of aero-engine key components manufacturing" [19] of regular crystalline alloys.

A highly interesting feature of the PECM method on BMGs is the ability to craft small parts from amorphous bulk material with material properties that stay unchanged from the casting conditions and

Table 2
Watchmaking standard NIHS 07-02 and R_a reached by common watchmaker polishing methods, where the crosses represent the typical achievable surface quality index N and the results of this study are marked with *.

	NIHS standard 07-02 (DIN EN ISO 1302)									
N class	N10	N9	N8	N7	N6	N5	N4	N3	N2	N1
max. R_a (μm)	12.5	6.3	3.2	1.6	0.8	0.4	0.2	0.1	0.05	0.025
Felt polishing						X	X	X	X	
Sandblasting			X	X	X	X	X			
Tumbling			X	X	X	X	X	X	X	
PECM (nano)*								X	X	X
PECM (BMG)*										X

following thermomechanical treatments prior to PECM. This will be the center of an application-based study on the manufacturing engineering capabilities of this novel, yet still conceptual fabrication route for BMG components.

Declaration of competing interest

The authors declare that they have no known competing financial interests or personal relationships that could have appeared to influence the work reported in this paper.

Acknowledgements

Instrumentation and technical assistance for this work were provided by the Service Center X-ray Diffraction, with financial support from Saarland University and German Science Foundation (project number INST 256/349-1). The authors thank Dr. Oliver Janka for the support in collection of the X-ray diffraction data presented in this paper and the help with the TOPAS analysis of the crystallite sizes for the respective primary phases. The authors acknowledge Instrumentation and technical assistance for this work that were provided by the Service Center Electron microscopy of Saarland University. Furthermore, we want to thank Jörg Schmauch for the provided Service of TEM imaging. The authors also thank the Heraeus AMLOY Technologies GmbH for providing the quality raw materials used for the synthesis of the high purity Vit105 alloy in this study.

Appendix A. Supplementary data

Supplementary data to this article can be found online at https://doi.org/10.1016/j.jmrt.2024.07.130.

References

[1] Kruzic JJ. Bulk metallic glasses as structural materials: a review. Adv Eng Mater 2016;18:1308–31. https://doi.org/10.1002/adem.201600066.
[2] Peker A, Johnson WL. A highly processable metallic glass: Zr41.2Ti 13.8Cu12.5Ni10.0Be22.5. Appl Phys Lett 1993;63:2342–4. https://doi.org/10.1063/1.110520.
[3] Grell D, Gibmeier J, Dietrich S, Silze F, Böhme L, Schulze V, Kühn U, Kerscher E. Influence of shot peening on the mechanical properties of bulk amorphous Vitreloy 105. Surf Eng 2017;33:721–30. https://doi.org/10.1080/02670844.2017.1282712.
[4] Bochtler B. Thermophysical and structural investigations of a CuTi- and a Zr-based bulk metallic glass, the influence of minor additions. and the relation to thermoplastic forming 2019. https://doi.org/10.22028/D291-31111.
[5] Gludovatz B, Naleway SE, Ritchie RO, Kruzic JJ. Size-dependent fracture toughness of bulk metallic glasses. Acta Mater 2014;70:198–207. https://doi.org/10.1016/j.actamat.2014.01.062.
[6] Jiang WH, Liu FX, Choo H, Liaw PK. Effect of structural relaxation on mechanical behavior of a Zr-based bulk-metallic glass. Mater Trans 2007:1781–4. https://doi.org/10.2320/matertrans.MJ200734.
[7] Kozak J, Zybura-Skrabalak M. Some problems of surface roughness in electrochemical machining (ECM). Procedia CIRP 2016;42:101–6. https://doi.org/10.1016/j.procir.2016.02.198.
[8] Guo C, Wu B, Xu Bin, Wu S, Shen J, Wu X. Investigation of pulse electrochemical machining of Zr-based bulk metallic glasses in NaNO 3 -ethylene glycol electrolyte. J Electrochem Soc 2021;168:071502. https://doi.org/10.1149/1945-7111/ac0bf8.
[9] Hall T, Adam B, Busch R, Bähre D. Pulse Electrochemical Machining of bulk metallic glasses. Proc. 18th Int. Symp. Electrochem. Mach. Technol. 2022:71–6.
[10] McCracken I, Busch R. Molding of fine surface features into bulk metallic glass. Mater Res Soc Symp - Proc 2003;806:399–404. https://doi.org/10.1557/proc-806-mm8.17.
[11] Kumar G, Staffier PA, Blawzdziewicz J, Schwarz UD, Schroers J. Atomically smooth surfaces through thermoplastic forming of metallic glass. Appl Phys Lett 2010;97. https://doi.org/10.1063/1.3485298.
[12] Frey M, Wegner J, Neuber N, Reiplinger B, Bochtler B, Adam B, Ruschel L, Riegler SS, Jiang HR, Kleszczynski S, Witt G, Busch R. Thermoplastic forming of additively manufactured Zr-based bulk metallic glass: a processing route for surface finishing of complex structures. Mater Des 2021;198:109368. https://doi.org/10.1016/j.matdes.2020.109368.
[13] Weber O, Natter H, Bähre D. Pulse electrochemical machining of cast iron: a layer-based approach for modeling the steady-state dissolution current. J. Solid State Electrochem. 2015;19(5):1265–76. https://doi.org/10.1007/s10008-014-2735-1.
[14] Nečas D, Klapetek P. Gwyddion: an open-source software for SPM data analysis. Cent Eur J Phys 2012;10:181–8. https://doi.org/10.2478/s11534-011-0096-2.
[15] Gates-Rector S, Blanton T. The Powder Diffraction File: a quality materials characterization database. Powder Diffr 2019;34:352–60. https://doi.org/10.1017/S0885715619000812.
[16] Bakradze G. Initial oxidation of zirconium: oxide-film growth kinetics and mechanisms. Ger: Univ. Stuttgart; 2011. p. 1–123. PHD Thesis.
[17] Wali A, Platt T, Meijer A, Biermann D. Micro structuring tool steel components using Precise Electrochemical Machining (PECM). Prod Eng 2023;17:473–81. https://doi.org/10.1007/s11740-022-01167-2.
[18] Mankeekar T, Bähre D, Durneata D, Hall T, Lilischkis R, Natter H, Saumer M. Fabrication of micro-structured tools for the production of curved metal surfaces by pulsed electrochemical machining. Int J Adv Manuf Technol 2022;119:2825–33. https://doi.org/10.1007/s00170-021-08146-4.
[19] Xu Z, Wang Y. Electrochemical machining of complex components of aero-engines: developments, trends, and technological advances. Chin J Aeronaut 2021;34:28–53. https://doi.org/10.1016/j.cja.2019.09.016.